

Auxiliary Material for

Relationships between outgoing longwave radiation and diabatic heating in reanalyses

Kai Zhang¹, William J. Randel², Rong Fu¹

¹ Jackson School of Geosciences, The University of Texas at Austin, Austin, Texas.

² National Center for Atmospheric Research, Boulder Colorado.

1. Introduction

The auxiliary material consists of five figures based on JRA-55 and MERRA2 reanalyses used for comparison with ERA-Interim results in the main text.

2. Auxiliary material

Fig. S1 Zonal mean diabatic heating averaged over the period of 1979-2013 for Q_{totoal} , $Q_{\text{radiation}}$, Q_{physics} , Q_{LW} and Q_{Sw} in JRA-55 (left panel) and MERRA2 (right panel), corresponding to Figure 3.

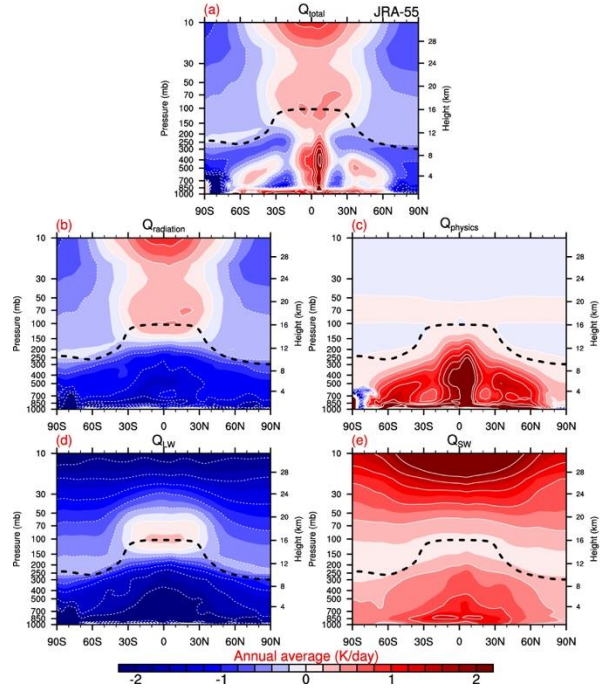
Fig. S2 Zonal-vertical correlation between OLR and anomalies of Q_{totoal} , $Q_{\text{radiation}}$, Q_{physics} , Q_{LW} and Q_{Sw} in JRA-55 (left panel) and MERRA2 (right panel), corresponding to Figure 5.

Fig. S3 Composite diabatic heating anomalies according to co-located OLR anomalies for Q_{totoal} , $Q_{\text{radiation}}$, Q_{physics} , Q_{LW} and Q_{Sw} over western Pacific (10°S - 10°N , 120° - 180°E) in JRA-55 (left two columns) and MERRA2 (right two columns), corresponding to Figure 8.

Fig. S4 Composite diabatic heating anomalies according to co-located OLR anomalies for Q_{totoal} , $Q_{\text{radiation}}$, Q_{physics} , Q_{LW} and Q_{Sw} over northwestern Pacific (30° - 50°N , 120° - 180°E) in JRA-55 (left two columns) and MERRA2 (right two columns), corresponding to Figure 9.

Fig. S5 Vertical profiles of cloud fraction, cloud liquid water content, and cloud ice water content composited according to co-located OLR, for statistics in the western Pacific and storm track regions in JRA-55 (left two columns) and MERRA2 (right two columns), corresponding to Figure 11.

JRA-55



MERRA2

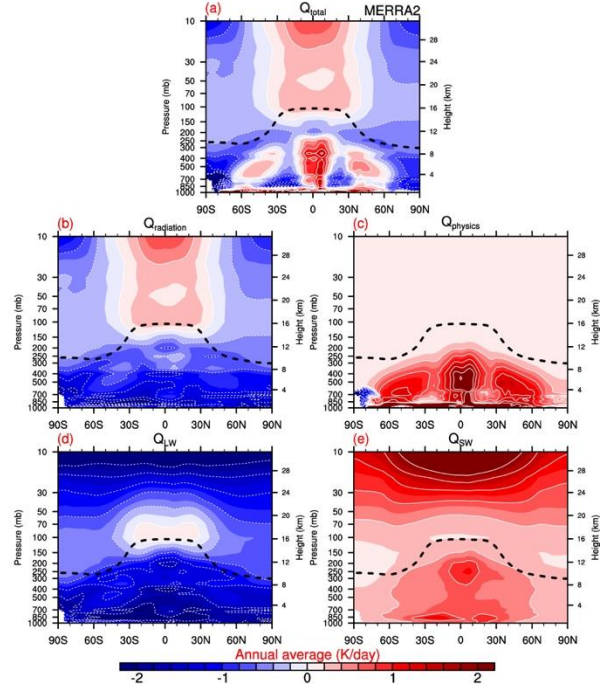


Fig. S1 Zonal mean diabatic heating averaged over the period of 1979-2013 for Q_{total} , $Q_{\text{radiation}}$, Q_{physics} , Q_{LW} and Q_{SW} in JRA-55 (left panel) and MERRA2 (right panel), corresponding to Figure 3.

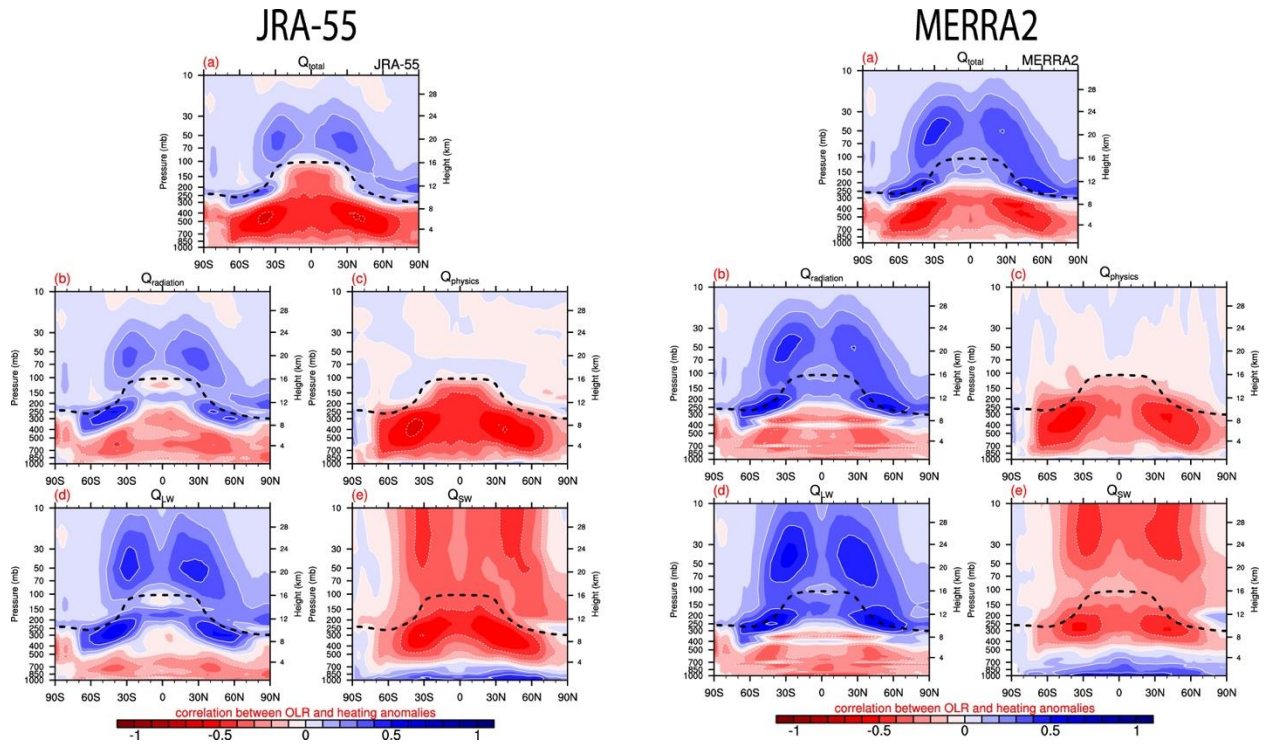
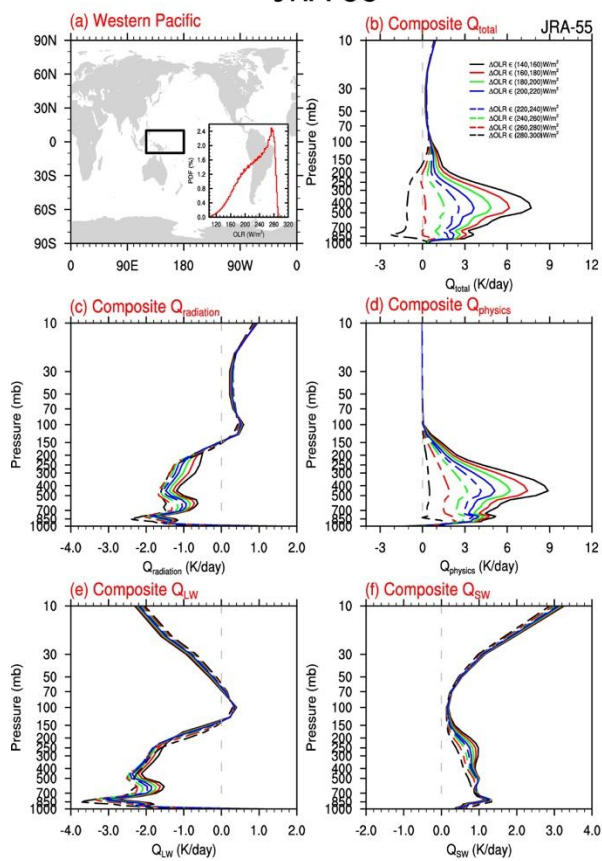


Fig. S2 Zonal-vertical correlation between OLR and anomalies of Q_{total} , $Q_{\text{radiation}}$, Q_{physics} , Q_{LW} and Q_{sw} in JRA-55 (left panel) and MERRA2 (right panel), corresponding to Figure 5.

JRA-55



MERRA2

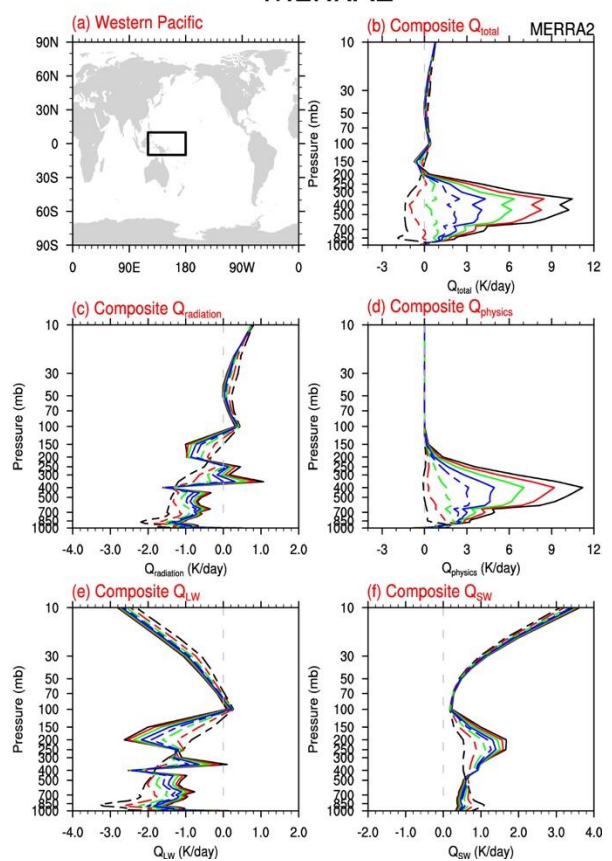
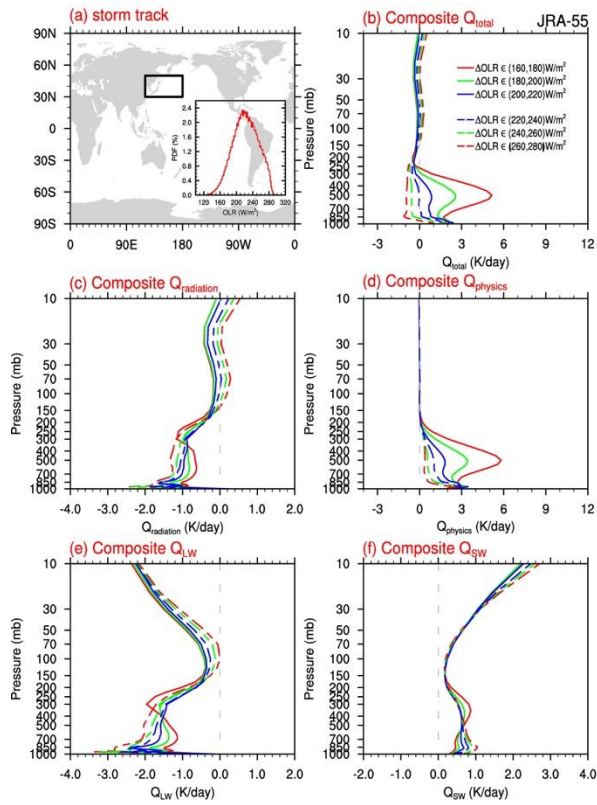


Fig. S3 Composite diabatic heating anomalies according to co-located OLR anomalies for Q_{total} , $Q_{\text{radiation}}$, Q_{physics} , Q_{LW} and Q_{SW} over western Pacific (10°S - 10°N , 120° - 180°E) in JRA-55 (left two columns) and MERRA2 (right two columns), corresponding to Figure 8.

JRA-55



MERRA2

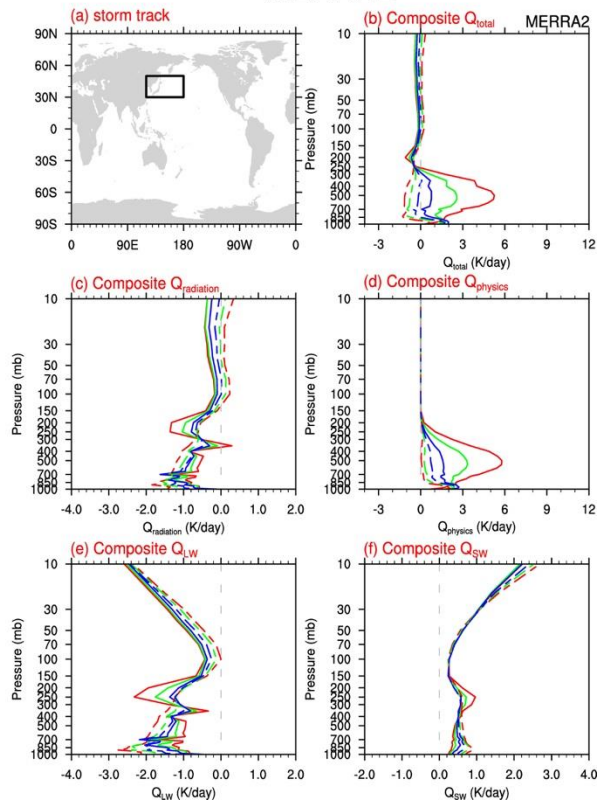
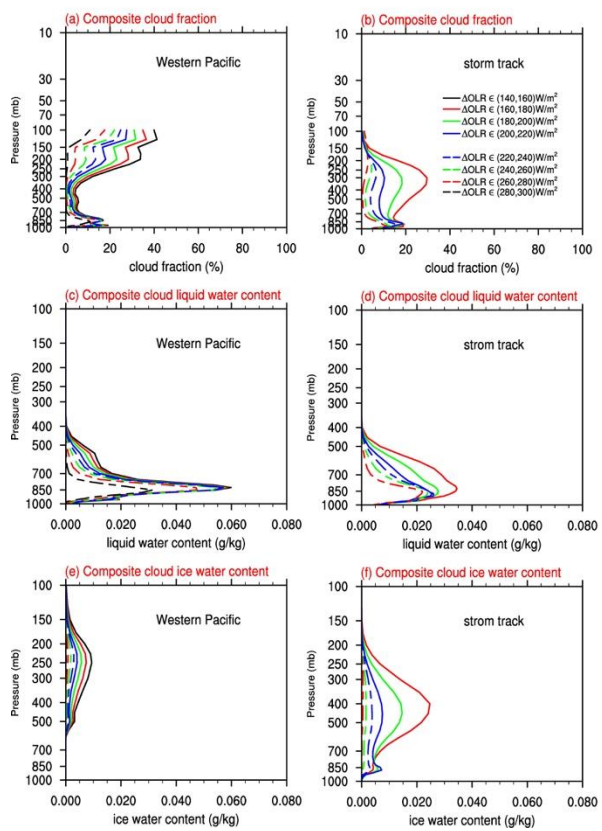


Fig. S4 Composite diabatic heating anomalies according to co-located OLR anomalies for Q_{total} , $Q_{\text{radiation}}$, Q_{physics} , Q_{LW} and Q_{SW} over northwestern Pacific (30°-50°N, 120°-180°E) in JRA-55 (left two columns) and MERRA2 (right two columns), corresponding to Figure 9.

JRA-55



MERRA2

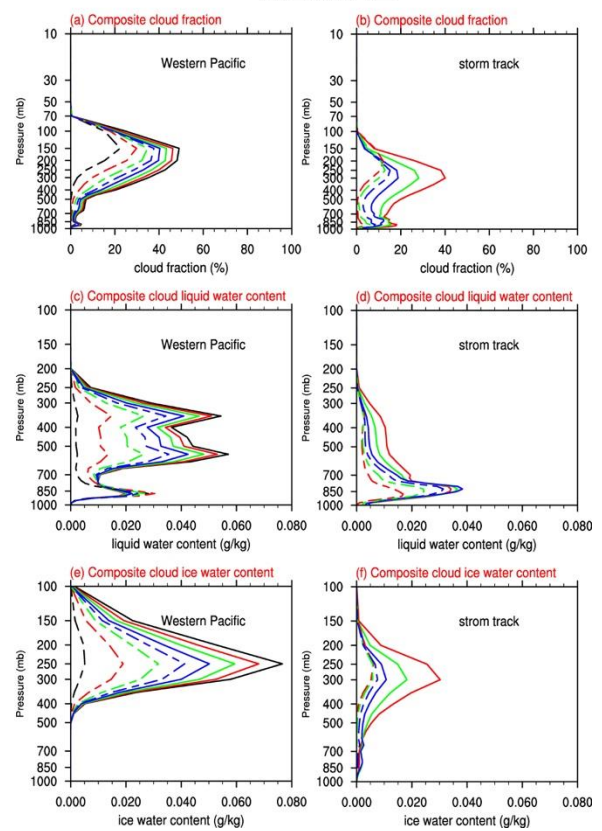


Fig. S5 Vertical profiles of cloud fraction, cloud liquid water content, and cloud ice water content composited according to co-located OLR, for statistics in the western Pacific and storm track regions in JRA-55 (left two columns) and MERRA2 (right two columns), corresponding to Figure 11.